ELSEVIER

Materials Science and Engineering A 398 (2005) 113–127

MATERIALS SCIENCE & ENGINEERING A

www.elsevier.com/locate/msea

Vacuum-furnace brazing of C103 and Ti–6Al–4V with Ti–15Cu–15Ni filler-metal

In-Ting Hong, Chun-Hao Koo *

Department of Materials Science and Engineering, National Taiwan University, No. 1, Sec. 4, Roosevelt Rd., Taipei, 106 Taiwan, ROC

Received 25 November 2004; received in revised form 1 March 2005; accepted 1 March 2005

Abstract

C103 and Ti–6Al–4V alloys joined by vacuum-furnace brazing using Ti–15Cu–15Ni (wt.%) commercial filler-metal was investigated. This study examines how brazing conditions affect the microstructural evolution and shear strength of the C103/TiCuNi/Ti–6Al–4V joint. According to the microstructural observations, all the characteristic structures of the joint interface can be classified into seven categories, based on their morphology and chemical composition. The microstructural morphology of each characteristic zone depends on the brazing time and the brazing temperature. Excessive increasing the brazing time and the brazing temperature form the coarse acicular Widmanstätten structure in front of Ti–6Al–4V parent-metal and cause grain growth of Ti–6Al–4V alloy. However, if the brazing time is too short or the brazing temperature is too low, the continuous intermetallic-layer consisting of intermetallic compounds, such as Ti_2(Cu, Ni) and Ti_2(Ni, Cu), will remain in the brazed joints after brazing. Additionally, during brazing, the diffusion of molten liquid filler-metal and the dilution of parent-metals cause the composition of the filler-metal to deviate from the Ti–Cu–Ni eutectic into the hypoeutectic or hypereutectoid. Therefore, the joint interface is anticipated to be comprised mostly of eutectic and/or eutectoid structures. The fine hypoeutectic and hypereutectoid structures consisting of α-Ti, Ti_2(Ni, Cu) and Ti_2(Cu, Ni) are observed in the joint interface brazed at 960 °C for 15 min. The maximum shear strength reaches 354 MPa under this brazing condition. Further increasing the brazing time and/or raising the brazing temperature cause excessive growth of the Widmanstätten structure and the grain of Ti–6Al–4V alloy, which significantly deteriorate the shear strength of joint. The high temperature shear strength of the C103/TiCuNi/Ti–6Al–4V joint was investigated to evaluate its limit service temperature. Moreover, the overlap-length and the joint clearance investigations are also conducted to realize the relations between different brazing conditions and the joint performance.

Keywords: Ti–6Al–4V; C103; TuCuNi filler-metal; Shear strength; Intermetallics; Vacuum-furnace brazing

1. Introduction

Niobium is a refractory metal with the lowest density. The melting point of pure niobium is 2468 °C, and pure niobium has excellent elevated-temperature strength even over 1300 °C [1–3]. Therefore, niobium-based alloys are widely applied in most major aerospace components due to their weight-saving properties compared with other numerous rocket engine designed metals, such as Ni-based superalloy. One specific Nb alloy, C103, is considered to be the most useful niobium-based alloy for high temperature propulsion systems because of its excellent welding properties and the elevated-temperature strength. Following intensive alloy development efforts during the 1960s space–race era, C103 was developed to replace the weak niobium-based alloys, such as Nb–1Zr, while retaining their desirable formability and welding properties. The nominal composition of C103 alloy comprises 1% Ti and 10% Hf (wt.%), with the balance of Nb metal. This Nb–Hf–Ti ternary alloy satisfies most rocket engine applications for temperature up to 1500 °C, because of its superior physical, thermal and mechanical properties [1–3].

Ti–6Al–4V is an α–β Ti alloys, which can be strengthened by various heat treatments, such as solid-solutioning or aging treatment. This Ti alloy has low density, high specific

* Corresponding author. Tel.: +886 2 27365527/23634097; fax: +886 2 23634562.
E-mail address: chkoo@ccms.ntu.edu.tw (C.-H. Koo).

0921-5093/$ – see front matter © 2005 Elsevier B.V. All rights reserved.
doi:10.1016/j.msea.2005.03.007

strength, excellent tensile strength and toughness. Moreover, Ti–6Al–4V also can be welded, machined and forged [1]. Therefore, Ti–6Al–4V plays a critical role in the recent development of propulsion materials for spacecraft applications or satellite launch systems.

Propulsion systems may include C103 and Ti–6Al–4V alloys [3]. Therefore, technologies for joining C103 and Ti–6Al–4V dissimilar alloys, such as brazing, diffusion bonding and laser welding, are extremely important for the development of rocket propulsion systems. Generally, most Ti alloy brazing has been performed using aluminum or silver-based filler-metals [6–8]. Although these filler-metals have good wettability, the mechanical properties and corrosion resistance of joints brazed using these filler-metals are insufficient. Otherwise, the service temperature of these brazed joints is limited to below 300 °C. Consequently, joints, which must sustain higher temperature, are also brazed using Ti-based filler-metals. Previous work indicates that Ti-based filler-metals can successfully braze Ti–6Al–4V [9–11,17]. On the other hand, according to the Ti–Nb binary phase diagram [4], Nb and Ti elements can be solid-soluted with each other very well and do not form any intermetallic phase [26]. This indicates that Ti-based filler-metals are also suitable candidates for brazing Nb-based alloy. Therefore, Ti-based filler-metals are highly promising for brazing C103 and Ti–6Al–4V alloy. The brazing foil, Ti–15Cu–15Ni (wt.%), is chosen as the filler-metal for brazing of C103 and Ti–6Al–4V in this study.

To date, only limited data, mostly on mechanical properties, can be obtained about niobium alloy joints using some commercial filler-metals [12,13]. Furthermore, the microstructural evolution and phase composition of niobium alloy joints have not been studied in detail. Therefore, this research concentrates on an approach to joining C103 and Ti–6Al–4V alloys via vacuum-furnace brazing using Ti–15Cu–15Ni (wt.%) foil as the brazing filler-metal. The microstructure, shear strength, X-ray analysis and solidification process of the brazed joint have been comprehensively studied to clarify the relations between the microstructure and the joint performance.

2. Experimental procedures

Sheets of C103 and Ti–6Al–4V alloys of 2 mm thickness were used as parent-metal for brazing in this study. The sheets were cut into 10 mm × 10 mm × 2 mm (for microstructural analysis) and 15 mm × 12 mm × 2 mm (for shear strength test) by wire-cutting for subsequent brazed joining. These specimens were then polished using wet SiC paper with 100-grit and put into an acetone bath for ultrasonic cleaning prior to brazing. A Ti–15Cu–15Ni (wt.%) brazing foil with 60 μm thickness was used as the brazing filler-foil. This commercial filler-metal is a clad-laminated brazing filler-metal, and has liquidus temperatures of 960 °C. The brazing foil was degreased in acetone prior to bonding. The specimens with filler-metal were assembled into a sandwich type fixed with the stainless steel clamp, and then were carefully placed into the vacuum-furnace. Furnace brazing was conducted under the vacuum of 1×10^{-6} Torr. Brazing temperature and holding time were varied from 960 to 1050 °C and from 5 to 20 min, respectively. The heating rate was 20 °C/min throughout the experiment. All specimens were preheated to 840 °C and holded at this temperature for 3 min before being heated up to the brazing temperature. After brazing, all the samples were furnace-cooled from the brazing temperature to room temperature. Following bonding, specimens were cut using a low speed diamond saw, and then were mounted and polished. The cross-sections of the brazed specimens were investigated using a Phillips XL-30 scanning electron microscope (SEM) with an accelerating voltage of 20 kV. The quantitative chemical composition analysis of the brazed joints was conducted using a JEOL JXL-8800M electron probe microanalyzer (EPMA) equipped with a wavelength dispersive spectrometer (WDS). The spot size of the EPMA was 1 μm and its operation voltage was 20 kV. To measure the bonding strength of brazed joints, the shear test was conducted with the Shimadzu AG-10 universal testing machine at a constant speed of 1 mm/min. The shear test specimens had a width of 15 mm with an overlap-length of 2 mm and a thickness of 2 mm. The phase analysis of the seven characteristic zones was carried out using a Philips PW 1710 X-ray diffractometer with Cu Kα radiation from 10° to 90°. To identify all phases of the seven characteristic zones, the specimen brazed

(a)

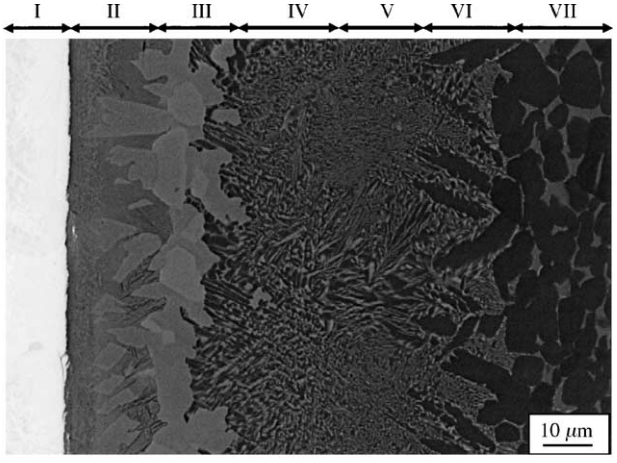

(b)

Element (wt.%)	Ti	Cu	Ni	Nb	Hf	Al	V
Zone I	1.1	0.0	0.0	89.1	9.8	0.0	0.0
Zone II	50.1	3.2	2.9	42.1	1.7	0.0	0.0
Zone III	62.2	22.8	14.1	0.6	0.1	0.1	0.1
Zone IV	83.4	8.5	7.2	0.1	0.0	0.5	0.3
Zone V	88.8	5.6	4.5	0.0	0.0	0.9	0.4
Zone VI	87.2	1.8	1.3	0.0	0.0	5.8	3.9
Zone VII	90.0	0.0	0.0	0.0	0.0	5.9	4.1

Fig. 1. (a) The microstructure of the C103/TiCuNi/Ti–6Al–4V joint brazed at 1000 °C for 5 min showing the seven characteristic zones of the cross-sectioned joint interface. (b) The EPMA analyses of the seven characteristic zones.

at 1000 °C for 5 min was cut parallel with the joint interface to remove most C103 parent-metal (Zone I, please see Fig. 1). The residual C103 parent-metal on the surface of the specimen was polished off by SiC paper of 2400 grit, so that the cross-section of Zone II appeared on the surface of the specimen and was identified by X-ray diffractometer. Following the X-ray analysis of Zone II, the specimen was polished gently to obtain the cross-section of the next zone (Zone III). The SEM was used to confirm what zone appeared on the surface of the specimen. X-ray analysis of each zone was conducted sequentially until the seven characteristic zones were all identified.

3. Results and discussion

3.1. Analysis of seven characteristic zones of the vacuum-furnace brazed C103/TiCuNi/Ti–6Al–4V joint

Fig. 1 shows a typical back-scattering electron image (BEI) of the C103/TiCuNi/Ti–6Al–4V joint interface brazed at 1000 °C for 5 min, and the chemical composition of each characteristic zone. This figure presents the complex microstructural transition from the parent-metal throughout the brazed joint. The characteristic microstructures are formed by atomic diffusion during the brazing, including diluting effect, isothermal solidification and solid-state diffusion occurring between each zone and the parent-metals [10,14,15]. In this study, all microstructures in the joint interface of specimens brazed on different brazing temperature and brazing time can be classified into seven characteristic zones based on their microstructural morphology and chemical composition. Fig. 2 shows higher-magnification microstructures of the seven characteristic zones in joint interface brazed at 1000 °C for 5 min. Fig. 3 displays the XRD results of the seven characteristic zones of the cross-sectioned joint interface brazed at 1000 °C for 5 min. These characteristic zones in Fig. 1 are nominated and discussed from left to right as follows:

(1) *Zone I, the C103 parent-metal area*: This zone is the C103 parent-metal area, and its chemical composition is Nb–10Hf–1Ti (wt.%). After brazing under any of the brazing conditions in this study, the microstructure of this zone is still unchanged. The unchanged microstructure implies that the brazing conditions, including the brazing temperature and the brazing time, are insufficient to change the microstructure of the C103 parent-metal or to promote the grain growth.

(2) *Zone II, the C103 reaction area*: This zone is the reaction area of the C103 parent-metal with the molten liquid filler-metal. During brazing, the dissolved elements of the C103 parent-metal react with molten liquid TiCuNi filler-metal in this area. This zone is a three-phases mixed region, as shown in Fig. 2(b). The EPMA analysis reveals that bright and gray phases are Nb-rich and Ti-rich phases, respectively. In addition, some acicular precipitates are present in this reaction area, when brazed under certain conditions, as shown in Fig. 2(b).

(3) *Zone III, the continuous intermetallic-layer*: Zone III, situated at the central region of the joint interface, is a continuous intermetallic-layer that diffuses incompletely during the brazing, as shown in Fig. 2(c). The total Ni amount (Ni plus Cu contents) in this zone is higher than those of the original Ti–15Cu–15Ni (wt.%) filler-metal. The EPMA analysis reveals that the chemical composition of this area is Ti–22.8Cu–14.1Ni (wt.%). This zone is the only complete liquid-phase throughout the joint interface before cooling because of its high Cu and Ni concentration. The continuous intermetallic-layer is only observed in specimens brazed at a low brazing temperature and/or for a short brazing time. The width of the continuous intermetallic-layer reduces as the brazing temperature and/or brazing time increases.

(4) *Zone IV, the hypoeutectic structure area*: The formation of Zone IV relates to a eutectic reaction of $L \rightarrow \alpha Ti + Ti_2(Cu, Ni) + Ti_2(Ni, Cu)$. However, the concentration of Cu and Ni in this area (Cu ∼ 8.5 wt.%, Ni ∼ 7.2 wt.%) is lower than those at the Ti–Cu–Ni ternary eutectic point, Ti–10.2Cu–20.1Ni (wt.%). Therefore, this area forms a hypoeutectic structure, as shown in Fig. 2(d). The EPMA and XRD results reveal that both black strip-like and black round phase with high Ti content are the α-Ti phase, and the white strip-like phase with high Cu and Ni contents is Ti_2(Ni, Cu) and/or Ti_2(Cu, Ni) intermetallic phase. This zone changes into Zone V as the brazing time is prolonged and/or the brazing temperature is raised.

(5) *Zone V, the hypereutectoid structure area*: The formation of Zone V differs slightly from that of Zone IV. This Zone V, the hypereutectoid structure area, forms by a eutectoid reaction of $\beta Ti \rightarrow \alpha Ti + Ti_2(Cu, Ni) + Ti_2(Ni, Cu)$. The isothermal diffusion of molten liquid filler-metal and the dilution of parent-metals that occur during brazing change the chemical composition of molten filler-metal, so that Zones IV and V have different chemical compositions and form different microstructural morphologies after cooling. Comparing the location of Zone V with that of Zone IV, as shown in Fig. 1, Zone V is closer to the Ti–6Al–4V parent-metal (Zone VII). Therefore, Zone V has lower Cu and Ni concentration (Cu ∼ 5.6 wt.%, Ni ∼ 4.5 wt.%) because of the greater dilution caused by the dissolving elements of Ti–6Al–4V parent-metal. This area forms a hypereutectoid structure after brazing, as shown in Fig. 2(e), and the width of this zone strongly depends on the brazing conditions.

(6) *Zone VI, the Widmanstätten structure area*: This zone is located between the hypereutectoid structure (Zone V) and the Ti–6Al–4V parent-metal (Zone VII). The Cu and Ni atoms of filler-metal diffusing into the Ti–6Al–4V parent-metal cause the β-transus temperature of Ti–6Al–4V to reduce below 990 °C. Therefore,

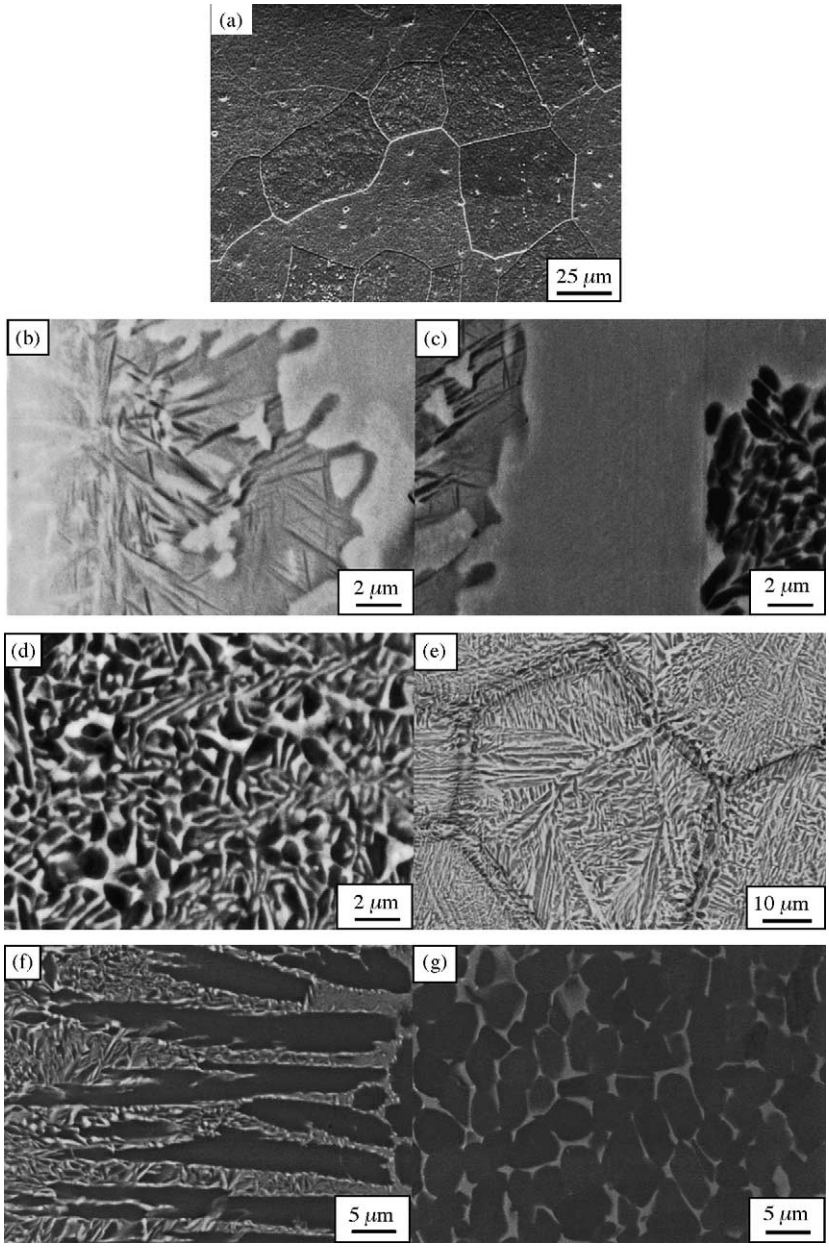

Fig. 2. The higher-magnification microstructures of the seven characteristic zones of the cross-sectioned joint interface brazed at 1000 °C for 5 min: (a) the C103 parent-metal area (Zone I), (b) the C103 reaction area (Zone II), (c) the continuous intermetallic-layer (Zone III), (d) the hypoeutectic structure area (Zone IV), (e) the hypereutectoid structure area (Zone V), (f) the Widmanstätten structure area (Zone VI) and (g) the Ti–6Al–4V parent-metal area (Zone VII).

the equiaxed α-Ti in the Ti–6Al–4V parent-metal wherein Cu and Ni atoms diffuse transforms into β-Ti during brazing, even at a brazing temperature below 990 °C. Under cooling, this β-Ti transforms into acicular α-Ti [17,25], as shown in Fig. 2(f). The EPMA and XRD results reveal that the acicular phase with a slight amount of Cu and Ni is the α-Ti phase.

(7) *Zone VII, the Ti–6Al–4V parent-metal area*: This zone is the Ti–6Al–4V parent-metal, which is composed of equiaxed α-Ti and intergranular β-Ti phases, as shown in Fig. 2(g). The dark and the bright phases are α-Ti and β-Ti phases, respectively. As brazing is conducted above the β-transus temperature of Ti–6Al–4V, the equiaxed α-Ti will transform into coarse plate-like α-Ti [1,25], which significantly deteriorates the ductility and shear strength of the joint.

3.2. Phase transformation and solidification process of the C103/TiCuNi/Ti–6Al–4V joint brazed at 1000 °C for 5 min

At the end of the brazing process, the high temperature phases that are present in the joint interface will transform into the room temperature phases. Each characteristic zone,

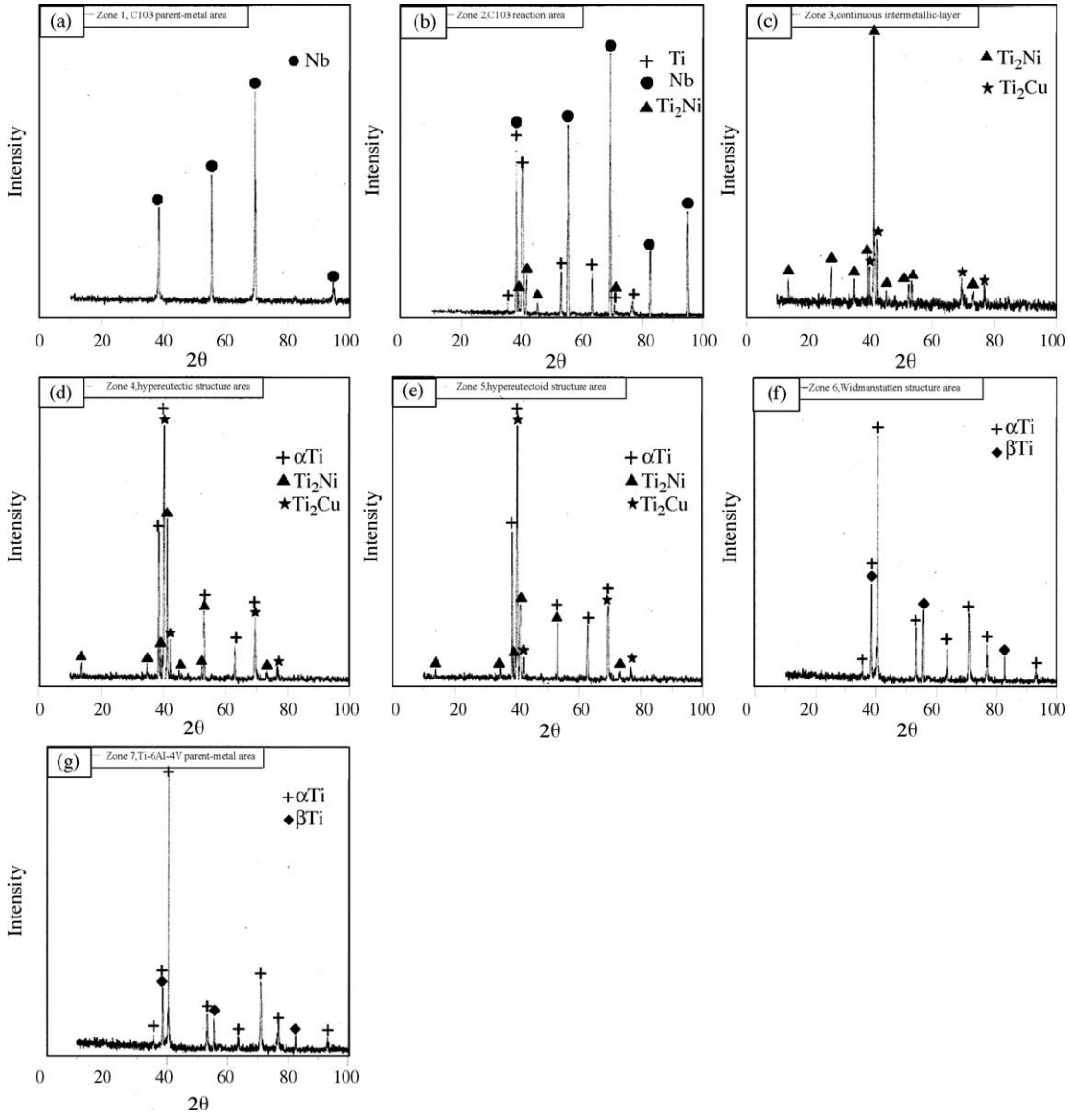

Fig. 3. The X-ray analysis of the seven characteristic zones of the cross-sectioned joint interface brazed at 1000 °C for 5 min: (a) the C103 parent-metal area (Zone I), (b) the C103 reaction area (Zone II), (c) the continuous intermetallic-layer (Zone III), (d) the hypoeutectic structure area (Zone IV), (e) the hypereutectoid structure area (Zone V), (f) the Widmanstätten structure area (Zone VI) and (g) the Ti–6Al–4V parent-metal area (Zone VII).

because of the different chemical composition, has a distinct solidification process and exhibits a different microstructural morphology. The solidification process and the phase transformation of each characteristic zone during cooling are discussed with different phase diagrams as follows. Additionally, Table 1 presents the phase transformations of the seven characteristic zones.

However, before the solidification process and the phase transformation of each characteristic zone will be discussed, some characteristics of Cu and Ni elements have to be realized. The Cu and Ni atoms are β-Ti stabilizers, and have similar atomic sizes. The atomic radii of Cu and Ni are 0.118 and 0.125 nm, respectively. They also have the same crystal structures (fcc). Both Cu and Ni may combine to form an isomorphous solid-solution [16,22]. Additionally, the microprobe analysis across the joint interface shows the complementary phenomena of Cu and Ni elements, as shown in Fig. 8. To discuss the solidification process of the continuous intermetallic-layer (Zone III), the hypoeutectic structure (Zone IV) and the hypereutectoid structure (Zone IV) in the joint interface from the pseudo Ti–(Ni, Cu) binary phase diagram, which can make up for some deficiencies of the ternary phase diagram, the characteristics of the Cu atoms are assumed to be similar to those of the Ni atoms [14,15,22]. This study obtains the total Ni amount by adding up the contents of Ni and Cu. Moreover, the isothermal section at 1013 °C of the Ti–Cu–Ni ternary system is similar to that of pseudo Ti–(Ni, Cu) binary system, as shown in Fig. 4(a) and the broken line in Fig. 4(b). These results reveal that the assumption made in this study is reasonable.

Table 1
The phase transformation of seven characteristic zones

	Zone numbers						
	I	II	III	IV	V	VI	VII
Phase category	C103 parent-metal	C103 reaction area	Continuous intermetallic-layer	Hypoeutectic structure	Hypereutectoid structure	Widmanstätten structure	Ti6A14V parent-metal
Phases at 1000 °C	β-(Nb, Hf) solid-solution	β-(Nb, Ti) solid-solution + Ti_2(Ni, Cu)	Molten liquid	β-Ti + liquid	β-Ti	β-Ti	α-Ti + β-Ti
Phases at 25 °C	β-(Nb, Hf) solid-solution	α-Ti + Nb-rich phase + Ti_2(Ni, Cu)	Ti_2(Ni, Cu) + Ti_2(Cu, Ni)	α-Ti + Ti_2(Ni, Cu) + Ti_2(Cu, Ni)	α-Ti + Ti_2(Ni, Cu) + Ti_2(Cu, Ni)	Acicular α-Ti + β-Ti	α-Ti + β-Ti

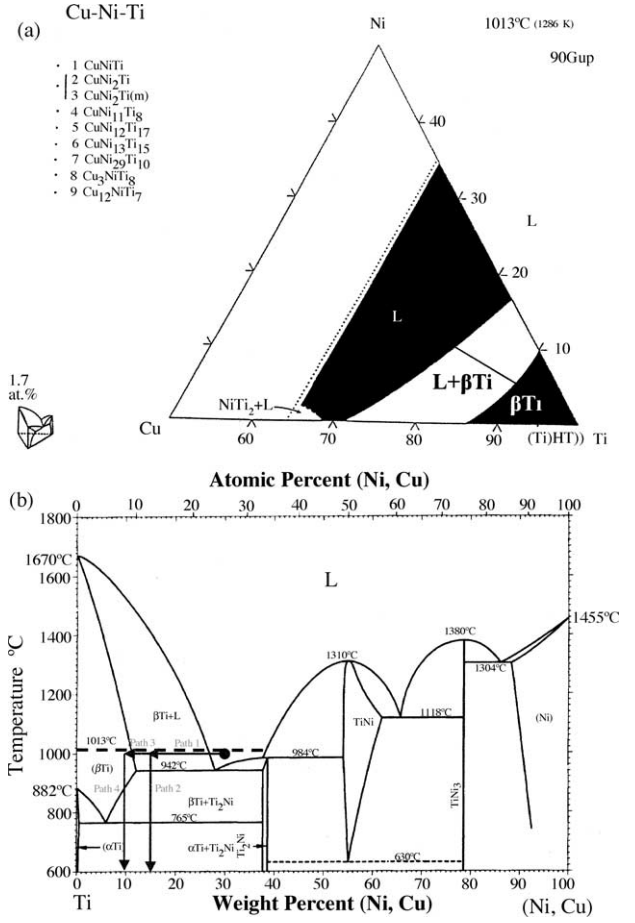

Fig. 4. (a) The 1013 °C isothermal section of the Ti–Cu–Ni ternary system. (b)The pseudo Ti–(Ni, Cu) binary phase diagram. There are four types of phase-transformation path produced by isothermal diffusion and dilution of parent-metals (paths 1 and 3), and cooling (paths 2 and 4). Mark (●) is the composition of original filler-metal.

(1) *Zone I*: As mentioned before, Zone I is the C103 parent-metal area. According to the Nb–Hf–Ti ternary phase diagram [5], Zone I is a single-phase in which niobium matrix solid-soluted with hafnium and titanium elements at 1000 °C. After cooling to room temperature, no precipitate forms in the niobium matrix, and this zone still maintains a single-phase. No microstructural change is observed in this zone after cooling, indicating that the brazing conditions are insufficient to change the microstructure or the grain size of the C103 parent-metal.

(2) *Zone II*: Zone II is the reaction area of the C103 parent-metal with molten liquid filler-metal. The C103 parent-metal dissolved slightly into the molten liquid filler-metal during brazing. One of the reasons for adding Cu and Ni into the filler-metal is to decrease the melting point of the filler-metal [17,18,21]. Once the C103 parent-metal partially dissolves into the molten liquid filler-metal and dilutes the Cu and Ni concentration of this zone, the melting point of the molten metal in Zone II raises, and that forces this zone to solidify before cooling. The chemical composition of this reaction area is 50.1% Ti, 43.8%

Nb (42.1% Nb and 1.7% Hf), 6.1% Ni (3.2% Cu and 2.9% Ni) in wt.%. According to the Nb–Ti–(Ni, Cu) ternary phase diagram [20], Zone II comprises of β-(Ti, Nb) solid-solution and Ti_2(Ni, Cu) and/or Ti_2(Cu, Ni) at 1000 °C. After cooling to room temperature, this area changes into a mixed region of three-phases consisting of the Ti-rich phase, the Nb-rich phase and intermetallic phase, such as Ti_2(Ni, Cu) and/or Ti_2(Cu, Ni), as shown in Figs. 2(b) and 3(b).

(3) *Zone III*: Zone III is the continuous intermetallic-layer. This zone contains higher total Ni amount (36.9 wt.%, the Ni and Cu contents are 14.1 and 22.8 wt.%, respectively) than the original filler-metal because of the segregation occurred during isothermal solidification [14,15]. Zone III is the only area that remains in a completely liquid state throughout the joint interface before cooling. According to the chemical composition and pseudo Ti–(Ni, Cu) binary phase diagram, as cooling from high temperature, the liquid phase solidifies by a reaction of $L \rightarrow Ti_2(Ni, Cu) + Ti_2(Cu, Ni)$ due to its high concentration of Cu and Ni. The XRD results reveal this zone is comprised of mainly large amounts of Ti_2(Ni, Cu) and/or Ti_2(Cu, Ni) intermetallic phases, as shown in Fig. 3(c). Removing the continuous intermetallic-layer is required to achieve sufficient joint strength. The region of continuous intermetallic-layer appears to undergo an excessively low brazing temperature or an excessively short brazing time. The width of the continuous intermetallic-layer reduces as the brazing temperature and/or the brazing time increases. When the specimens are brazed at 960 or 1000 °C, the continuous intermetallic-layer areas disappear within brazing times of 15 or 10 min, respectively.

(4) *Zone IV*: During brazing, especially at a high temperature, the parent-metal is fused and dissolved into the molten liquid filler-metal, and that is inevitable [19]. Therefore, upon the filler-metal melts, the isothermal diffusion of liquid filler-metal and the dilution of Ti–6Al–4V parent-metal would occur in Zones IV and V. Zones IV and V exhibit different morphologies of microstructures because of their different chemical compositions. Zone IV near the continuous intermetallic-layer has a hypoeutectic structure owing to its high total Ni amount (15.7 wt.%, the Ni and Cu contents are 7.2 and 8.5 wt.%, respectively). On the contrary, Zone V near the Ti–6Al–4V parent-metal side shows a hypereutectoid structure because of its low total Ni amount (10.1 wt.%, the Ni and Cu contents are 4.5 and 5.6 wt.%, respectively).

The TiCuNi filler-metal melts into a liquid and diffuses towards both sides of the parent-metal when the brazing temperature exceeds its melting point. The EPMA analysis reveals that the total Ni amount in Zone IV approaches 16 wt.% (Ni ∼ 7.2 wt.%, Cu ∼ 8.5 wt.%). The pseudo Ti–(Ni, Cu) binary phase diagram, as shown in Fig. 4(b), indicates the solidification process of this area. Before cooling, some β-Ti first precipitate from the molten liquid phase because the Cu and Ni concentration of this zone is diluted by the Ti–6Al–4V parent-metal, as depicted by path 1 in Fig. 4(b). These β-Ti are proeutectic phase. During cooling, the remnant liquid phase with a hypoeutectic composition solidifies and forms a lamellate hypoeutectic structure, as depicted by path 2 in Fig. 4(b). Upon cooling to room temperature, the round and lamellate β-Ti are transformed into α-Ti. Fig. 2(d) shows the black round and lamellate α-Ti, and the bright lamellate Ti_2(Ni, Cu) or Ti_2(Cu, Ni).

(5) *Zone V*: As mentioned above, during brazing the parent-metals dissolve into the molten liquid filler-metal [19]. The Cu and Ni concentration of Zones IV and V are lower than those of Zone III because the dissolving element of Ti–6Al–4V parent-metal dilutes the molten liquid filler-metal in Zones IV and V. The total Ni amount of Zone V is lower than that of Zone IV because Zone V is closer to the Ti–6Al–4V parent-metal than Zone IV. Therefore, the total Ni amount in this area is more strongly diluted by the dissolving elements of Ti–6Al–4V parent-metal than those in Zone IV. The EPMA analysis shows that the total Ni amount of this area is diluted to approximately 10 wt.% (Cu ∼ 5.6 wt.%, Ni ∼ 4.5 wt.%). The pseudo Ti–(Ni, Cu) binary phase diagram in Fig. 4(b) indicates the solidification process of this area. Before cooling, the molten liquid phase in this zone is completely solidified into β-Ti, as shown in Fig. 4(b) by path 3. During the subsequent solidification, Ti_2(Ni, Cu) and/or Ti_2(Cu, Ni) precipitate along the grain boundary of β-Ti [16]. These precipitates are proeutectoid phase. Upon cooling to room temperature, β-Ti is transformed into a laminated structure, which consists of α-Ti, Ti_2(Ni, Cu) and Ti_2(Cu, Ni), through the hypereutectoid reaction of $\beta\text{-Ti} \rightarrow \alpha\text{-Ti} + Ti_2(Ni, Cu) + Ti_2(Cu, Ni)$, as shown in Fig. 4(b) by path 4. The hypereutectoid structure is extremely fine and is not easy to be observed using SEM with a low magnification. However, with a high magnification of about over 6500, the lamellate structure of the bright Ti_2(Ni, Cu) and Ti_2(Cu, Ni) phases and the black α-Ti phase would be observed. This structure produces a sufficiently strong brazed joint, as discussed in Section 3.4. The formation of the lamellate structure in this zone is similar to the formation of the eutectic structure. The Cu and Ni atoms must be rearranged by diffusion during phase transformation due to the different composition of matrix from that of the precipitated phases. The diffusional distance of the Cu and Ni atoms is minimized by the formation of this lamellate structure [16], in which the α-Ti, Ti_2(Ni, Cu) and/or Ti_2(Cu, Ni) form after cooling.

Additionally, according to the pseudo Ti–(Ni, Cu) binary phase diagram, the hypoeutectoid structure appears in the joint interface as the total Ni amount of the joint interface decreases to below 5 wt.%. However, this kind of structure would not be observed in this study because the total Ni amount of the joint interface is difficult

to decrease from 30 to 5 wt.% just by brazing under the conditions in this study. According to the EPMA analysis, the total Ni amount of the joint interface brazed at 1050 °C for 20 min (the highest brazing temperature and the longest brazing time in this study) is 6.1 wt.% (Cu ∼ 3.2 wt.%, Ni ∼ 2.9 wt.%), which is higher than the hypoeutectoid point. Therefore, the hypereutectoid structure is formed in the joint interface, instead of forming the hypoeutectoid structure.

(6) *Zone VI*: This zone is the acicular Widmanstätten structure area. During brazing, the Cu and Ni elements diffuse to the front of the Ti–6Al–4V parent-metal and reduce its β-transus temperature. Therefore, the α-Ti matrix wherein the Cu and Ni elements diffuse, transforms into the β phase during brazing. As cooling, the β phase transforms back into the α phase and forms the acicular Widmanstätten structure [17]. The acicular α phase has lower ductility than the equiaxed α phase. Although the acicular α phase can blunt the crack tip and stop crack propagation, it generates cracks more easily than does the equiaxed α phase because of its long interface [1,16]. Therefore, the coarse, acicular Widmanstätten structure should be avoided during brazing.

(7) *Zone VII*: This zone is the Ti–6Al–4V parent-metal area. The Cu and Ni elements of the filler-metal cannot diffuse into this zone to reduce the β-transus temperature because this area is far from the TiCuNi molten liquid filler-metal. Therefore, the β-transus temperature of this area remains at 990 °C. In case of brazing below the β-transus temperature, such as 960 °C, this zone still maintains the equiaxed α phase after brazing. In contrast, when brazed above the β-transus temperature, this zone transforms into the β phase during brazing, and then into coarse plate-like α-Ti phase as it cools to room temperature.

3.3. Microstructural evolution of the vacuum-furnace brazed C103/TiCuNi/Ti–6Al–4V joint

Fig. 5(a–d) shows the SEM back-scattered electron images (BEI) of the C103/TiCuNi/Ti–6Al–4V joints brazed at 960 °C for 5, 10, 15 and 20 min, respectively. The composition of the TiCuNi filler-metal is close to that of the Ti–Cu–Ni ternary eutectic point. During brazing, the diffusion of molten liquid filler-metal and the dilution of parent-metals cause the composition of the liquid filler-metal to deviates to hypoeutectic or hypereutectoid, as shown in Fig. 4(b). Therefore, the joint interface is anticipated to be comprised mostly of eutectic and/or eutectoid structures. Microstructural observations reveal that both the brazing time and the brazing temperature significantly affect the microstructural evolution.

The seven characteristic zones, as mentioned above, coexist in the joint interface of the specimen brazed at 960 °C for 5 min, as shown in Fig. 5(a). The continuous intermetallic-layer that consists of intermetallic phases, such as Ti_2(Cu, Ni) and/or Ti_2(Ni, Cu), is observed in the central region of the brazed joint because of the short brazing time. The hypoeutectic (Zone IV) and hypereutectoid (Zone V) structures form in the region adjacent to the central continuous intermetallic-layer. These two structures are believed to result from the Ti–6Al–4V parent-metal dissolving into the molten liquid filler-metal and diluting the Cu and Ni concentrations of the liquid filler-metal. Only traces of the acicular Widmanstätten

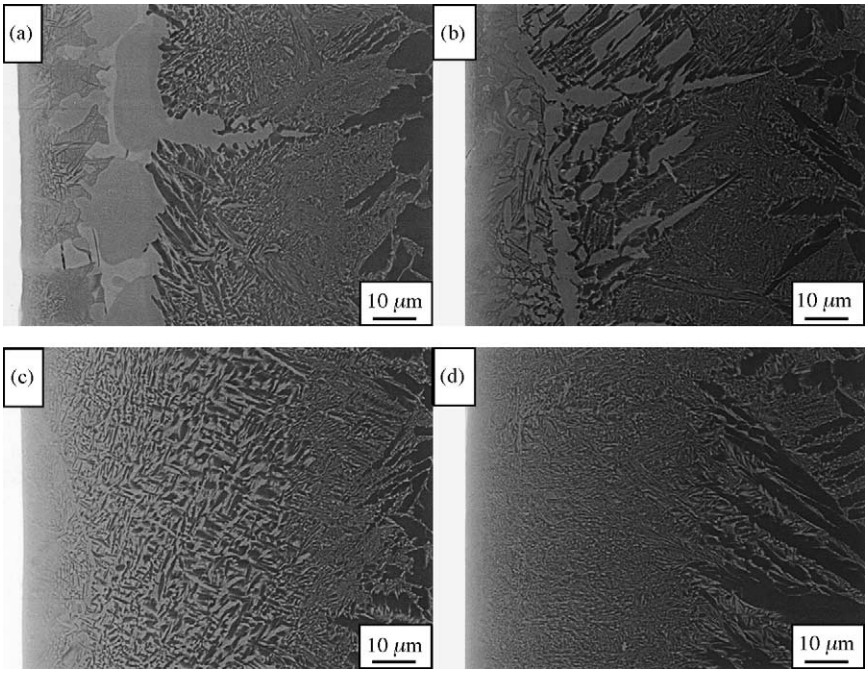

Fig. 5. The back-scattering electron images (BEIs) of the C103/TiCuNi/Ti–6Al–4V specimens brazed at 960 °C for (a) 5 min, (b) 10 min, (c) 15 min and (d) 20 min.

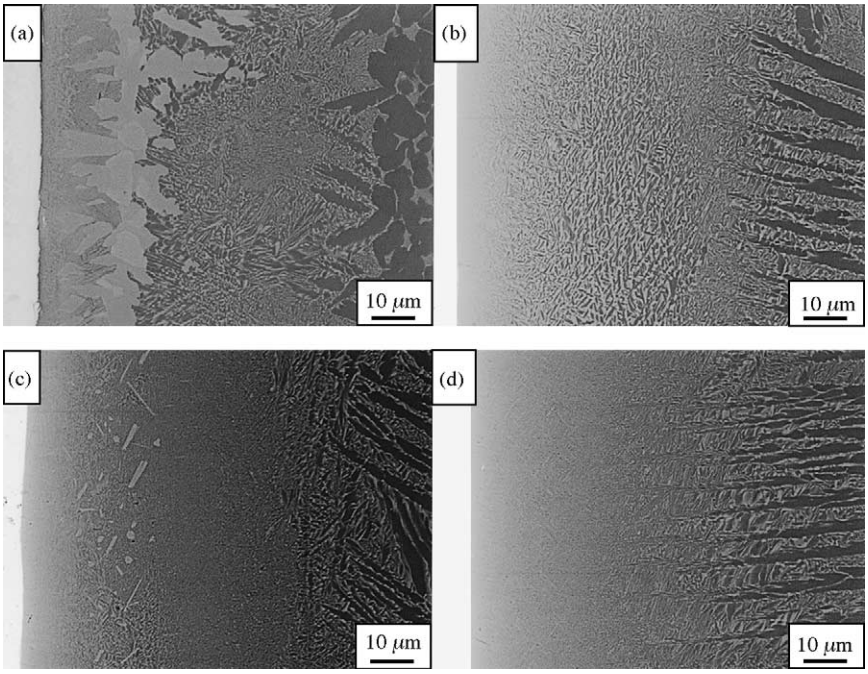

Fig. 6. The back-scattering electron images (BEIs) of the C103/TiCuNi/Ti–6Al–4V specimens brazed at 1000 °C for (a) 5 min, (b) 10 min, (c) 15 min and (d) 20 min.

structure in the joint interface are observed, because the Cu and Ni elements have not diffused into the Ti–6Al–4V parent-metal yet. Some acicular phases can be observed in the C103 reaction area (Zone II).

When the brazing time is extended to 10 min, the width of the continuous intermetallic-layer reduces to 3 μm, as shown in Fig. 5(b). In this case, the continuous intermetallic-layer is surrounded by the dark phases in the joint interface. The EPMA analysis reveals that the dark phase is a Ti-rich phase, which precipitated from the liquid filler-metal before cooling. The amount of tiny acicular phases existing in Zone II reduces as the brazing time is prolonged. The microstructural morphology of the other zones did not clearly change as the brazing time is prolonged from 5 to 10 min.

When the brazing time is increased to 15 min, the continuous intermetallic-layer disappears because the elements of the filler-metal are all sufficiently diffused. In this case, the joint interface is mainly comprised of the C103 reaction area (Zone II), the hypoeutectic (Zone IV) and the hypereutectoid (Zone V) structures. No coarse Widmanstätten structure exists in the joint interface. This combined microstructures provide the brazed joints with the maximum shear strength, 354 MPa, as mentioned in Section 3.4.

When the brazing time is extended to 20 min, the degree of dissolution of the parent-metals into the molten filler-metal is enhanced. The total Ni amount of all filler-metals are diluted to a lower level (about 10 wt.%), as shown in Fig. 8(b), at which only the hypereutectoid structure (Zone V) can be formed. Meanwhile, the coarse Widmanstätten structure is formed in this joint because the Cu and Ni atoms have diffused into the Ti–6Al–4V parent-metal, reducing its β-transus temperature. Therefore, in this case, the joint interface consists of the C103 reaction area (Zone II), the hypereutectoid (Zone V) and the acicular Widmanstätten (Zone VI) structures. The hypoeutectic structure (Zone IV) in this joint interface disappeared because the total Ni amount of the molten filler-metal was reduced by the dilution of parent-metals.

Fig. 6(a–d) shows the SEM back-scattered electron images (BEI) of the C103/TiCuNi/Ti–6Al–4V joints brazed at 1000 °C for 5, 10, 15 and 20 min, respectively. Fig. 6(a) reveals that the seven characteristic zones still coexist in the joint interface of the specimen brazed at 1000 °C for 5 min, but their microstructural morphologies are somewhat changed due to the raising brazing temperature. Fig. 6(a) shows that the continuous intermetallic-layer remains in the joint interface, but its width is reduced to about 3 μm. Some acicular Widmanstätten structure can be observed in the specimen brazed at 1000 °C for 5 min because the brazing temperature has exceeded the β-transus temperature. Further prolonging the brazing time extends the acicular Widmanstätten structure and changes the hypoeutectic structure (Zone IV) into the hypereutectoid structure (Zone V).

Fig. 7(a–d) shows the SEM back-scattered electron images (BEI) of the C103/TiCuNi/Ti–6Al–4V joints brazed at 1050 °C for 5, 10, 15 and 20 min, respectively. According to the aforementioned microstructural observations, the continuous intermetallic-layer exists in the joint interface of the specimens brazed at 960 or 1000 °C for 5 min. However, the continuous intermetallic-layer disappears within 5 min as the brazing temperature is raised to 1050 °C. The hypereutectoid and hypoeutectic structures can be still observed in the joint due to the difference of the Cu and Ni concentrations

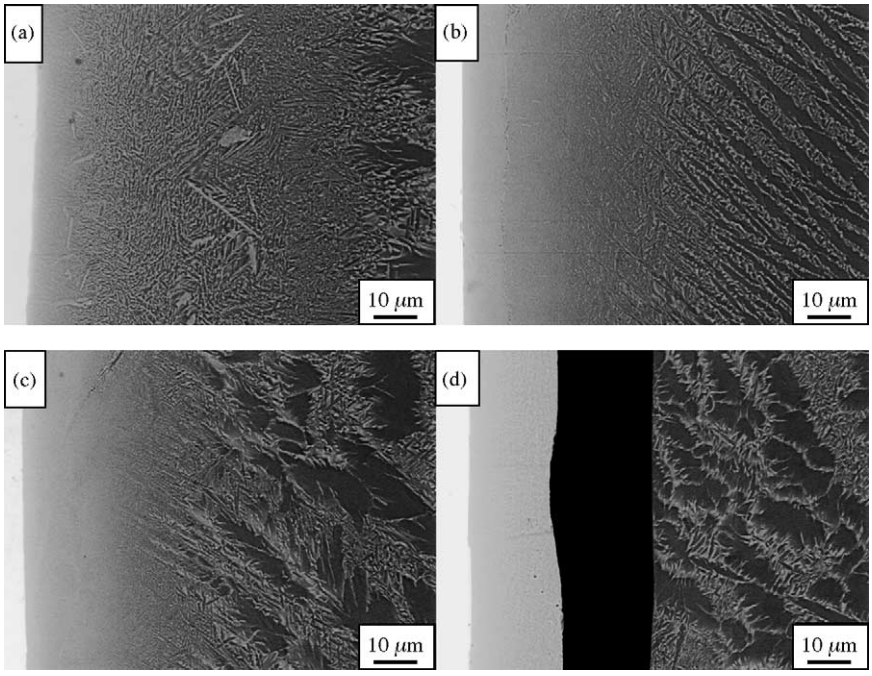

Fig. 7. The back-scattering electron images (BEIs) of the C103/TiCuNi/Ti–6Al–4V specimens brazed at 1050 °C for (a) 5 min, (b) 10 min, (c) 15 min and (d) 20 min.

in the joint interface. The acicular Widmanstätten structure appears to be larger and coarser than the one of specimens brazed at 960 and 1000 °C because of the diffusion of Cu and Ni elements and the overhigh brazing temperature. Further prolonging the brazing time causes the disappearance of the hypoeutectic structure, the formation of more acicular Widmanstätten structure and the grain coarsening in the matrix of Ti–6Al–4V, as well as the formation of cracks. The worst joint microstructure in the brazed specimens, from the mechanical perspective, is that in which containing continuous intermetallic-layer, coarse Widmanstätten structure and cracks.

3.4. Mechanical properties of the vacuum-furnace brazed C103/TiCuNi/Ti–6Al–4V joint

Fig. 9 shows the shear strength of the C103/TiCuNi/Ti–6Al–4V joints plotted against brazing time at different brazing temperatures. As a result, the shear strength of the specimen brazed at 960 °C for 5 min is insufficient. But the specimen brazed at the same temperature for 15 min has the maximum shear strength of 354 MPa. Further prolonging the brazing time to 20 min may reduce its shear strength to 298 MPa.

The joint brazed at 960 °C for 5 min with a low shear strength of less than 300 MPa fractures in the continuous intermetallic-layer (Zone III), as shown in Fig. 10(a). The XRD analysis of the C103 part of fracture surface confirms that the surface mainly comprises intermetallic phases, such as Ti_2(Cu, Ni) and/or Ti_2(Ni, Cu). These analytical results demonstrate that the continuous intermetallic-layer, which consists of brittle intermetallic compounds, deteriorates the shear strength of the joints.

As the brazing time is extended to 15 min, the continuous intermetallic-layer, which consists of continuous intermetallic compounds, disappears and changes into the hypoeutectic structure (Zone IV), as shown in Fig. 5(c). The intermetallic phase, such as Ti_2(Cu, Ni) and/or Ti_2(Ni, Cu), in Zone V is discontinuous. No continuous intermetallic phase exists in the joint interface after cooling. The maximum shear strength, 354 MPa, can thus be obtained under such a brazing condition. The fracture location changes from the continuous intermetallic-layer to the interface near the C103 parent-metal when the brazing time increasing from 5 to 15 min, as shown in Fig. 10(a and b).

As the brazing time is increased to 20 min, the hypoeutectic structure (Zone IV), which exists in the specimen brazed at 960 °C for 15 min, disappears and changes into the hypereutectoid structure (Zone V). Microstructural observations reveal that the hypereutectoid structure is finer than the hypoeutectic structure, and by conjecture, thus the shear strength of this joint should be higher than those of the joints brazed at 960 °C for 15 min. However, the testing results reveal that the shear strength reduces from 354 to 298 MPa as the brazing time is increased from 15 to 20 min. This result may be attributed to the formation of a large amount of coarse acicular Widmanstätten structure in the joint interface during brazing, as shown in Fig. 5(d).

It is to be noted that, after 5 min, the shear strength reduces with the increasing brazing time as the brazing temperature rises to 1050 °C. The evolution of shear strength of the specimen brazed at 1050 °C differs markedly from that

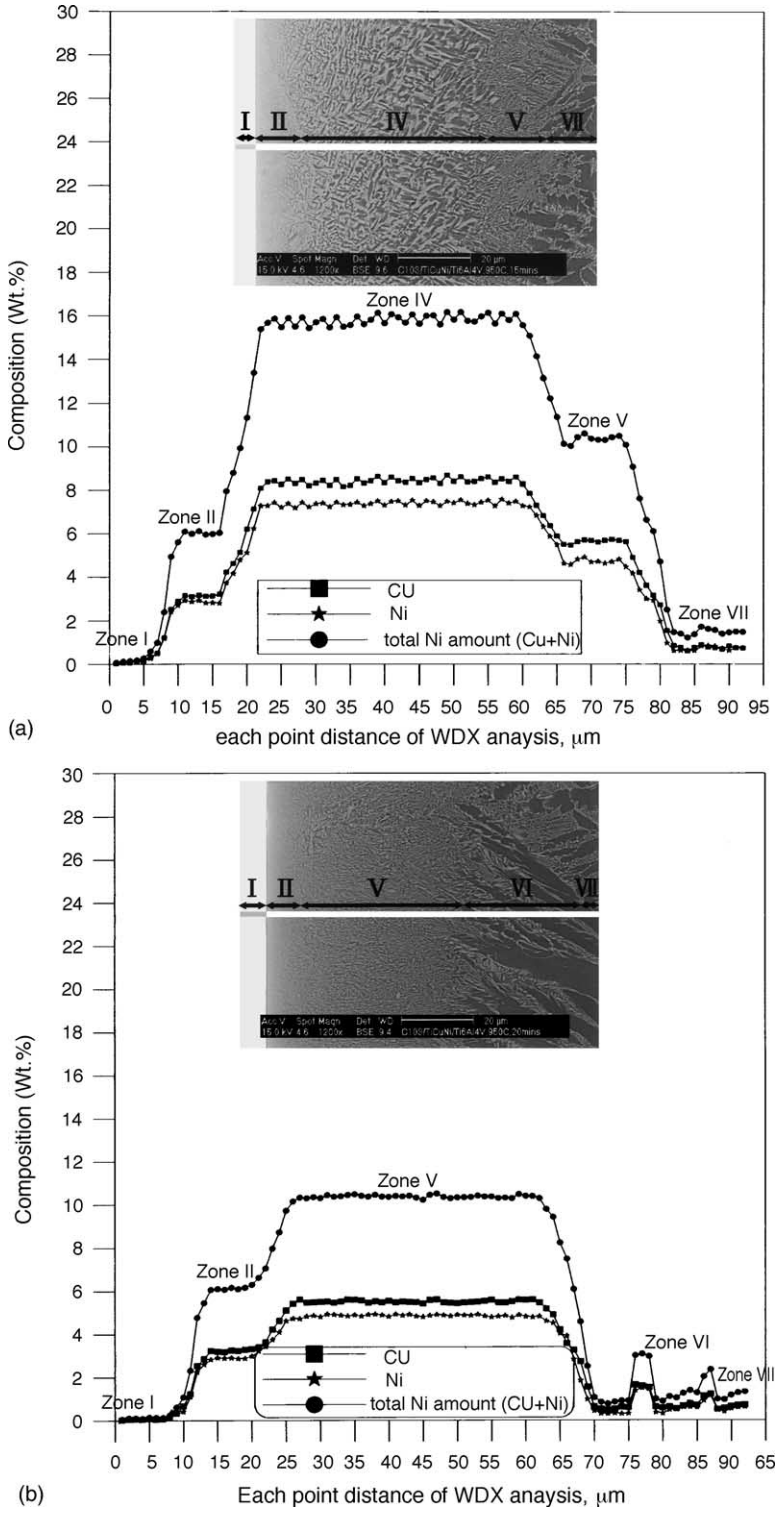

Fig. 8. (a) Microprobe analysis across the centre of the C103/TiCuNi/Ti–6Al–4V joint brazed at 960 °C for 15 min. (b) Microprobe analysis across the centre of the C103/TiCuNi/Ti–6Al–4V joint brazed at 960 °C for 20 min.

of the specimens brazed at 960 or 1000 °C. The microstructural observations reveal that no continuous intermetallic-layer exists in the joint interface of specimens brazed at 1050 °C, even if the brazing time is only 5 min. However, all the Ti–6Al–4V parent-metal transform into the acicular Widmanstätten structure because the brazing temperature exceeds the β-transus temperature. Further prolonging the brazing time makes the Widmanstätten structure become longer and coarser. When the brazing time extends to 20 min, the joint interface exhibits a lot of large voids. These microstructural ob-

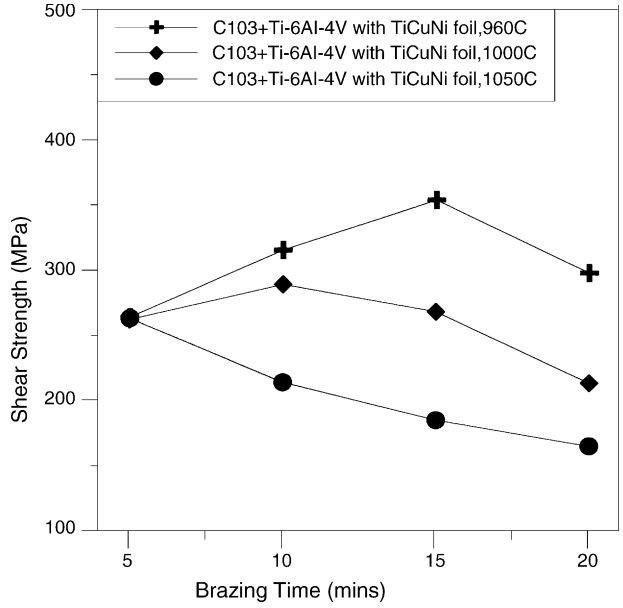

Fig. 9. The shear strength of the C103/TiCuNi/Ti–6Al–4V joint brazed under various brazing conditions.

servations reveal that increasing the brazing time at 1050 °C may promote the formation of a coarse Widmanstätten structure and the coarse grains of Ti–6Al–4V, and also may form large cracks in the joint interface. This is the reason why the shear strength of the specimen brazed at 1050 °C reduces with the brazing time extends, as shown in Fig. 9.

3.5. High temperature shear testing of the C103/TiCuNi/Ti–6Al–4V joint

Fig. 11 shows the high temperature shear strength of the C103/TiCuNi/Ti–6Al–4V joint, indicating that the shear strength of the C103/TiCuNi/Ti–6Al–4V joint can be maintained around 300 MPa or above at a temperature below 600 °C. However, the joint shear strength declines significantly as the temperature exceeds 600 °C, for the following reasons: (1) At a temperature above 600 °C, the joint interface between the C103 and Ti–6Al–4V parent-metals oxidizes seriously, reducing the shear strength of the joint. (2) As the test temperature rises to 800 °C, the joint strength significantly decreases to 10 MPa because the test temperature approaches the melting point of the TiCuNi filler-metal. These are the two main causes of the negative dependence of the joint shear strength on the temperature. Accordingly, the limit service temperature of the C103/TiCuNi/Ti–6Al–4V joint is below 700 °C. Exceeding the limit service tem-

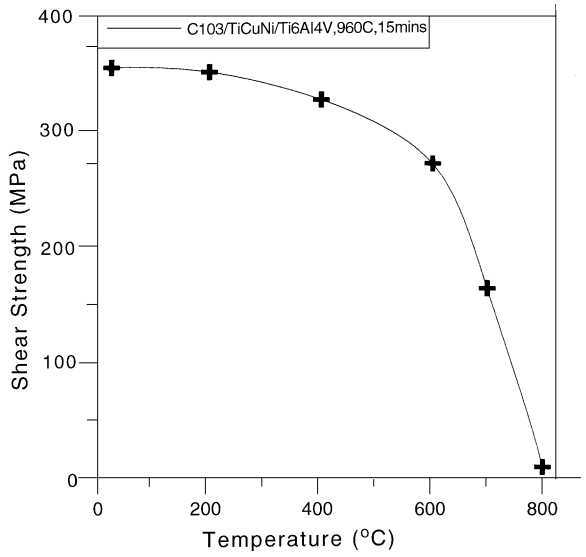

Fig. 11. The high temperature shear strength of the C103/TiCuNi/Ti–6Al–4V joint brazed at 960 °C for 15 min.

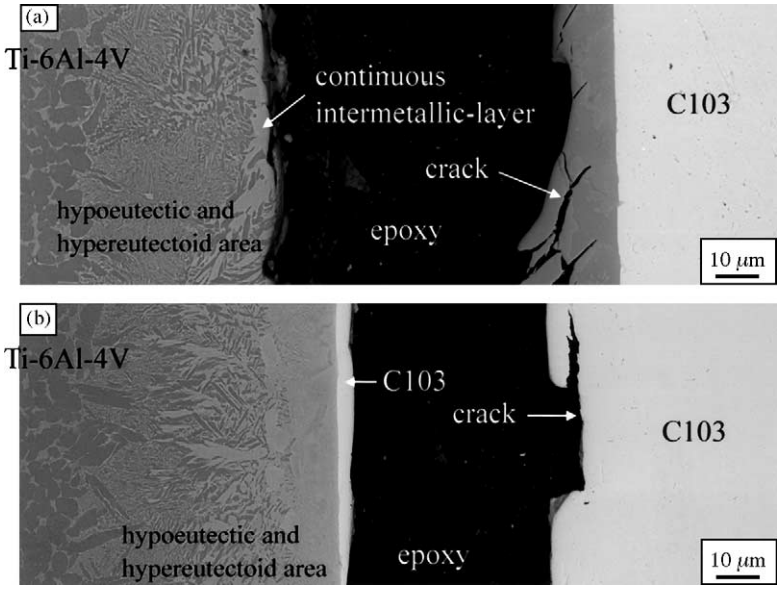

Fig. 10. The cross-section of the C103/TiCuNi/Ti–6Al–4V joint after shear test brazed at 960 °C for (a) 5 min and (b) 15 min.

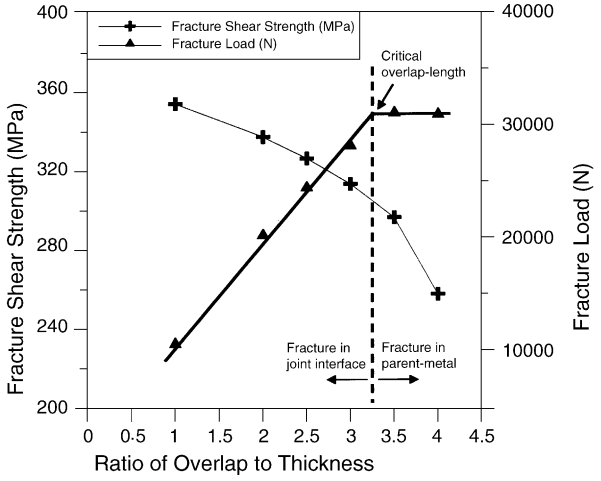

Overlap distance	1T (2mm)	2T (4mm)	2.5T (5mm)	3T (6mm)	3.5T (7mm)	4T (8mm)
Overlap area(mm^2)	30	60	75	90	105	120
Fracture Load(N)	10613	20217	24451	28165	31076	30920
Fracture Shear strength (MPa)	354	337	326	313	296	257

Fig. 12. Correlation diagram between shear strength and overlap-distance of the C103/TiCuNi/Ti–6Al–4V joint brazed.

perature causes the joints to failure under low loading.

3.6. Overlap-length investigation of the C103/TiCuNi/Ti–6Al–4V joint

The shear strength or tensile strength of the brazed joint depends mainly on its overlap-length. Too small an overlap-length causes the brazed joint to fail below the required loading, whereas too large an overlap-length means an unnecessarily wasteful material. Generally, the brazed joint with an overlap-length of three to five times the thickness of the parent-metals can achieve the maximum load-bearing capacity [26]. However, a large number of tests must be conducted to optimize the overlap-length for a specific brazed joint.

Fig. 12 is the correlation diagram between the fracture load, shear strength and the overlap-length of the brazed joint. The fracture load of the joint with an overlap-length of 2 mm, which is one time the thickness of parent-metal, is as low as 10,613 N because of its short overlap-length. The load-bearing capacity of the brazed joint generally increases with the overlap-length or overlap-area. As a result, the fracture load of the joint rises to 28,165 N as its overlap-length increases to three times the thickness of the parent-metal (3 T, 6 mm). Further increasing the overlap-length to three and a half times the thickness of the parent-metal (3.5 T, 7 mm) raises the fracture load to as high as 31,076 N, and the brazed joint fractures in C103 parent-metal. In Fig. 12, the point of intersection between the horizontal line and the oblique line is the critical overlap-length of the joint, and this value is about 3.2. Restated, the load-bearing capacity of the C103/TiCuNi/Ti–6Al–4V joints reaches the maximum, and

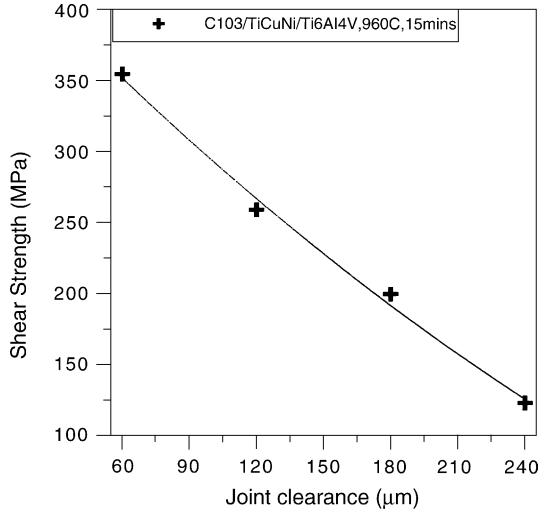

Fig. 13. Correlation diagram between shear strength and the joint clearance of the C103/TiCuNi/Ti–6Al–4V joint.

the brazed joint fractures in the C103 parent-metal when the overlap-length of the joint approaches 3.2.

Additionally, the fracture shear strength for each overlap-length was calculated as the failure load divided by the overlap-area, as shown in Fig. 12. The trend of the shear strength reduction with the increase of the overlap-length is different from that of the fracture load. This phenomenon had been discussed in some references [27–30], in which the Von Mises stress is utilized to demonstrate the decreasing of the joint shear strength. As the overlap-length of joint increases, the Von Mises stress distribution becomes less and less uniform during shear test. The middle portion of the overlap contributes less and less to the overall load-carrying capacity of the joint, whereas the ends of the joint become "overloaded". The non-uniform stress distribution in the lap joint causes the decreasing of the shear strength [28,29].

3.7. Joint clearance investigation of C103/TiCuNi/Ti–6Al–4V joint

An appropriate clearance for a brazed joint depends not only on the properties of filler-metal, but also on the surface roughness of parent-metals, the interaction between the parent-metals and the filler-metal, and the brazing process [26]. Fig. 13 plots the relation between the joint clearance and the shear strength of the C103/TiCuNi/Ti–6Al–4V joint, indicating that the shear strength of the joint declines as the joint clearance increases. A joint clearance of 60 μm can achieve the maximum shear strength because a smaller joint clearance increases capillarity, and thus the distribution of the filler-metal throughout the joint area, and reduces the formation of voids or shrinkage cavities in the joint as the filler-metal solidifies.

Moreover, the amount of continuous intermetallic-layer in the joint interface increases with the increasing of joint clearance, as shown in Fig. 14. The continuous intermetallic-layer,

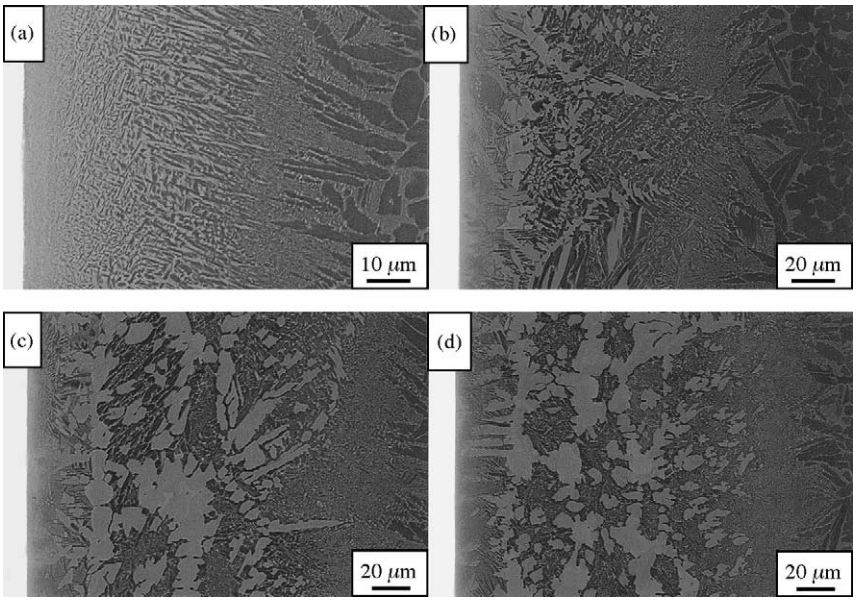

Fig. 14. The microstructure of the C103/TiCuNi/Ti–6Al–4V joint with different joint clearances: (a) 60 μm, (b) 120 μm, (c) 180 μm and (d) 240 μm.

which consists of brittle intermetallic compounds, causes the decreasing of shear strength.

4. Conclusions

(1) Experimental observations reveal that all the microstructures of the joint interface can be classified into seven characteristic zones. The microstructural morphology of the joint gradually changes as the brazing time or brazing temperature increases. The appearance of these microstructures and their effects on the corresponding shear strength depend strongly on the brazing conditions.

(2) During brazing, the parent-metals would dissolve into the molten liquid filler-metal. Therefore, the total Ni amount (Ni plus Cu contents) of molten liquid filler-metal in each zone decrease owing to the dilution of the parent-metal. Each zone has a different chemical composition and forms a different microstructural morphology. In this study, the diffusion of Cu and Ni atoms from the TiCuNi filler-metal into the parent-metals and the dilution of parent-metals are the main factors that control the microstructural morphology of the joint interface.

(3) The maximum shear strength is obtained when the joint interface comprises the C103 reaction zone, the hypereutectoid and the hypoeutectic structures. The brazed joints with shear strengths less than 300 MPa fractured in the continuous intermetallic-layer because of the brittleness of the continuous intermetallic phases. The C103/TiCuNi/Ti–6Al–4V joint brazed at 960 °C for 15 min was found to have joint strength of approximately 360 MPa. Further prolonging the brazing time causes the formation of the acicular Widmanstätten structure, which could decrease the shear strength to a low value below 300 MPa. Moreover, the shear strength of the C103/TiCuNi/Ti–6Al–4V joint can be maintained around 300 MPa at a temperature below 600 °C. As the temperature exceeds 600 °C, the shear strength of the joint markedly declines.

(4) Continuous intermetallic-layer, coarse acicular Widmanstätten structure, coarse Ti–6Al–4V grains and cracks form in the joint interface of the specimens brazed under inappropriate brazing conditions, and all of which markedly deteriorate shear strength of joints.

(5) The fracture load of joint raises with the increasing of the overlap-length. The critical overlap-length of the C103/TiCuNi/Ti–6Al–4V joint is around 3.2. The joint shear strength decreases with the increasing of the overlap-length because of the non-uniform stress distribution during shear test.

(6) For the C103/TiCuNi/Ti–6Al–4V joint, the joint shear strength decreases with the increasing of the joint clearance. The joint clearance maintained at about 60 μm can maximize the joint shear strength.

Acknowledgement

The authors gratefully acknowledge the financial support of this research by National Science Council (NSC), Republic of China, under the grants NSC 92-2623-7-014-012.

References

[1] W.F. Smith, Structure and Properties of Engineering Alloys, New York, 1993.

[2] J.R. Davis, Metals Handbook, Properties and Selection: Nonferrous Alloys and Special Purpose Materials, vol. 2, Ohio, ASM International, Materials Park, 1990.

[3] J.J. Stephens, JOM, August 1990, p. 22.
[4] T.B. Massalski, Binary Alloy Phase Diagrams, ASM International, Materials Park, 1990.
[5] P. Villars, A. Prince, H. Okamoto, Handbook of Ternary Alloy Phase Diagrams, ASM International, Materials Park, OH, 1995, p. 9848.
[6] R.K. Shiue, S.K. Wu, S.Y. Chen, Intermetallics 11 (2003) 661.
[7] R.K. Shiue, S.K. Wu, S.Y. Chen, Acta Mater. 51 (2003) 1991.
[8] W.T. Kaarlela, W.S. Margolis, Weld. J. 10 (1974) 629.
[9] O. Botstein, A. Schwarzman, A. Rabinkin, Mater. Sci. Eng. A206 (1995) 14.
[10] A. Hirose, M. Nojiri, H. Ito, K.F. Kobayashi, Int. J. Mater. Prod. Technol. 13 (1998) 13.
[11] O. Botstein, A. Rabinkin, Mater. Sci. Eng. A188 (1994) 305.
[12] T.J. Moore, Weld. Res. Suppl. 3 (1990) 98.
[13] G.K. Watson, T.J. Moore, Weld. J. 56 (1977) 306.
[14] S.J. Lee, S.K. Wu, R.Y. Lin, Acta Mater. 46 (1998) 1283.
[15] S.J. Lee, S.K. Wu, R.Y. Lin, Acta Mater. 46 (1998) 1297.
[16] R. Hill, E. Robert, Physical Metallurgy Principles, PWS-Kent Publisher, Boston, 1992.
[17] S.W. Lan, Weld. J. 10 (1982) 23.
[18] T. Onzawa, A. Suzumura, M.W. Ko, Weld. Res. Suppl. 10 (1990) 462.
[19] X.P. Zhang, Y.W. Shi, Scripta Mater. 50 (2004) 1003.
[20] Y. Guanjun, H. Shiming, J. Alloys Compd. 297 (2002) 226.
[21] A. Rabinkin, H. Liebermann, S. Pounds, T. Taylor, Scripta Mater. 25 (1991) 399.
[22] C.A. Blue, R.A. Blue, R.Y. Lin, Scripta Mater. 32 (1995) 127.
[25] D.F. Neal, Titanium'80 Sci. Technol. 1 (1981) 105.
[26] Ernest F. Nippes, Metals Handbook, Welding, Brazing and Soldering, vol. 6, ASM International, 1990.
[27] N. Bredzs, F.M. Miller, Weld. J. 11 (1968) 481.
[28] E. Lugscheider, H. Reimann, O. Knotek, Weld. J. 6 (1997) 189.
[29] Y. Flom, L. Wang, Weld. J. 7 (2004) 32.
[30] C.W. Shaw, L.A. Shepard, J. Wulff, Trans. ASM 57 (1964) 94.